ISSN (Print) 1226-1750
ISSN (Online) 2233-6656
Journal of Magnetics 23(4), 659-664 (2018) https://doi.org/10.4283/JMAG.2018.23.4.659

Circulating Current Analysis for High-Speed Motors with Stranded Windings by Considering End and Temperature Effect

Yapeng Jiang, Junquan Chen, Xuan Teng, and Dong Wang*

National Key Laboratory of Science and Technology on Vessel Integrated Power System, Naval University of Engineering, Wuhan, China

(Received 14 July 2018, Received in final form 13 December 2018, Accepted 17 December 2018)

This paper presents an improved circuit model for predicting additional copper loss caused by circulating current effect. Based on basic circuit equations and winding topology, this model takes account of both slot and end leakage inductance which are separately extracted by 2-D and 3-D finite element method. Several simplified windings are wounded in a stator to validate the accuracy of the proposed model. The results shows that this model has high accuracy and the maximum error of loss factor is about 1.5 %. In addition, it is found that the circulating current loss factor will decrease as the end winding length grows up or winding temperature increases.

Keywords : motor, AC copper loss, circulating current, electromagnetic-thermal coupling, end leakage inductance

1. Introduction

High-speed motors usually adopt stranded windings instead of form-wound windings for minimizing the skin and proximity effect. Due to the thin diameter of the strand, the current distribution in one strand can be regarded as uniform. Meanwhile, the linked leakage flux of each strand at different positions in one coil differs from each other, this leads to the uneven distribution of currents between different strands. The additional AC ohmic loss caused by the circulating current effect is considerable, especially for low-voltage high-speed motors [1, 2].

The issue of circulating current has attracted attention recently. Henry Hämäläinen has evaluated the AC resistance of a Litz wire and one-layer form-wound winding by finite element analysis (FEA), this method can also be applied to stranded windings [3, 4] despite its modeling and computation cost. Besides, papers that concentrate on this problem frequently adopt basic circuit equations with the assumption that the permeability of the core material is infinite and the current distribution in strand is uniform. Jiancheng Fang has modelled the circulating current by basic circuit equations and analyzed the geometrical influence factors of circulating current [2]. Strands transposition process can be used to eliminate circulating current effect. Martin van der Geest has estimated circulating current by basic circuit equations and analyzed the effects of strand displacements and twisting by 3-D FEA [5, 6]. Patel. B. Reddy has studied the effects of transposition of the insulated strands in stator winding bundles on the copper losses of high-speed machines, and 360° transposition over the length of the slots is shown to produce the lowest losses [8, 9]. To consider the randomness of strands placement, A. Lehikoinen has proposed a method by combining Monte Carlo method and basic circuit equations [10].

In general, the key to solve circulating current problem by basic circuit equations is the extraction of the impedance matrix. Most papers have only taken account of the slot leakage inductance without considering the end leakage inductance, which might bring a certain amount of calculation error. Besides, the resistance of each strand is partially determined by the extension length of end winding and winding temperature. The effects of these two factors on circulating current also needs to be investigated.

Based on basic circuit equations and incidence matrix, this papers aims to propose an improved circuit method

*Corresponding author: Tel: +86-13971105036
Fax: +86-027-65461969, e-mail: wangdongl@vip.sina.com

This paper was presented at the IcAUMS2018, Jeju, Korea, June 3-7, 2018.

by modifying the impedance matrix using end leakage inductance of end winding. The leakage parameters of end winding will be extracted by 3-D FEM method. The accuracy of the proposed method will be verified under different frequencies (200 Hz~5 kHz) and the effects of the end extension length and temperature on circulating current will be investigated.

2. Improved Circuit Model of Circulating Current

As shown in Fig. 1, the term *strand* refers to a single sub-conductor in a slot and the term *path* refers to a single sub-conductor of a phase. Here we ignore the non-linearity of the core material and its magnetic relative permeability is set as 10000. The current distribution inside the strand is assumed uniform.

The voltage equation in one slot including n_s strands can be expressed as $\boldsymbol{U}=\boldsymbol{ZI}$ where $\boldsymbol{U}$, $\boldsymbol{I}$ denote the voltage and current vector, and $\boldsymbol{Z}$ denotes the impedance matrix of all strands in one slot. The elements of the impedance matrix can be expressed as

$$\boldsymbol{Z}(i,k)=\begin{cases} r_e + r_s + j\omega L_{ii} & if\ i=k \\ j\omega L_{ik} & if\ i\neq k \end{cases} \tag{1}$$

where r_e, r_s respectively denote the end and slot part of DC resistance of one strand. L_{ik} denotes the mutual inductance between strand #i and strand #k. The temperature dependence of strand resistivity is to a great degree linear and can be described by the approximation below.

$$\rho(T)=\rho_0\left[1+\alpha\left(T-T_0\right)\right] \tag{2}$$

where $\rho(T)$, ρ_0 respectively denote the copper resistivity at temperature T and reference temperature T_0, α denotes the temperature coefficient of resistivity (copper, –0.393 %).

For the entire stator, the impedance matrix $\boldsymbol{Z}_{all}$ of all strands can be expressed as

$$\boldsymbol{Z}_{all}=\begin{bmatrix} \boldsymbol{Z} & \boldsymbol{Y}_{12} & \cdots & \boldsymbol{Y}_{1i} & \cdots & \boldsymbol{Y}_{1w} \\ \boldsymbol{Y}_{21} & \boldsymbol{Z} & \cdots & \boldsymbol{Y}_{2i} & \cdots & \boldsymbol{Y}_{2w} \\ \vdots & \vdots & & \vdots & & \vdots \\ \boldsymbol{Y}_{i1} & \boldsymbol{Y}_{i2} & \cdots & \boldsymbol{Z} & \cdots & \boldsymbol{Y}_{iw} \\ \vdots & \vdots & & \vdots & & \vdots \\ \boldsymbol{Y}_{w1} & \boldsymbol{Y}_{w2} & \cdots & \boldsymbol{Y}_{wi} & \cdots & \boldsymbol{Z} \end{bmatrix} \tag{3}$$

where $\boldsymbol{Y}_{ik}$ denotes the mutual impedance matrix between the strands in slot #i and slot #k. According to the winding topology, the impedance matrix $\boldsymbol{Z}_p$ of all paths can be expressed as

$$\boldsymbol{Z}_p=\boldsymbol{C}\boldsymbol{Z}_s\boldsymbol{C}^T \tag{4}$$

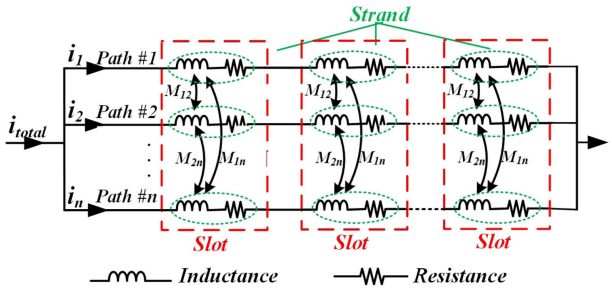

Fig. 1. (Color online) Schematic diagram of path and strand.

where $\boldsymbol{C}$ denotes the oriented incidence matrix between path and strand.

$$\boldsymbol{C}(p,i)=\begin{cases} 1, & \text{current in strand \#}i\text{ flows forward in path \#}p \\ -1, & \text{current in strand \#}i\text{ flows backward in path \#}p \\ 0, & \text{otherwise} \end{cases} \tag{5}$$

Considering the end leakage impedance matrix $\boldsymbol{Z}_e$ of all paths, the impedance matrix $\boldsymbol{Z}_p$ can be revised to $\boldsymbol{Z}_{pr}=\boldsymbol{Z}_p+\boldsymbol{Z}_e$.

For a typical 3-phase winding, the incidence matrix $\boldsymbol{F}$ between phase and path can be shown as

$$\boldsymbol{F}=\boldsymbol{E}_{3\times 3}\otimes\underbrace{\begin{bmatrix}1 & \cdots & 1\end{bmatrix}^T}_{n_p/3} \tag{6}$$

where n_p denotes the number of paths and the symbol $\otimes$ represents the Kronecker product. If the phase current vector $\boldsymbol{I}_{ph}$ is known as $[i_a\ i_b\ i_c]^T$, the phase voltage vector $\boldsymbol{U}_{ph}$ and the path current vector $\boldsymbol{I}_p$ can be expressed as

$$\boldsymbol{U}_{ph}=(\boldsymbol{F}^T\boldsymbol{Z}_{pr}^{-1}\boldsymbol{F})^{-1}\boldsymbol{I}_{ph} \qquad \boldsymbol{I}_p=\boldsymbol{Z}_{pr}^{-1}\boldsymbol{F}\boldsymbol{U}_{ph} \tag{7}$$

To show the circulating current influence on total copper loss, the circulating current loss factor k_f of n_p paths is defined as

$$k_c=\frac{n_p\sum_{k=1}^{n_p}\left|i_k\right|^2}{\left|\sum_{k=1}^{n_p}i_k\right|^2} \tag{8}$$

3. Parameters Extraction

In order to research conveniently, several simplified windings have been wounded in a stator for investigating circulating current problem as shown in Fig. 2. Parameters of the stator core is shown in Table 1. Among these windings, the red marked winding and five blue marked windings are respectively used to investigate the temperature and end effect. For each winding, there are two parallel paths with sixteen strands wounded at several fixed locations in four slots as shown in Fig. 3. Path #1 and path #2 respectively represent the path near the slot

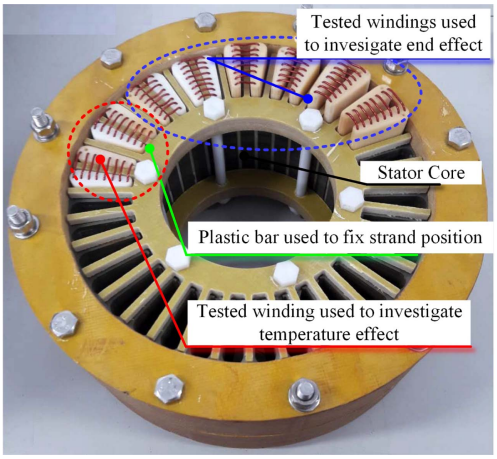

Fig. 2. (Color online) Tested model.

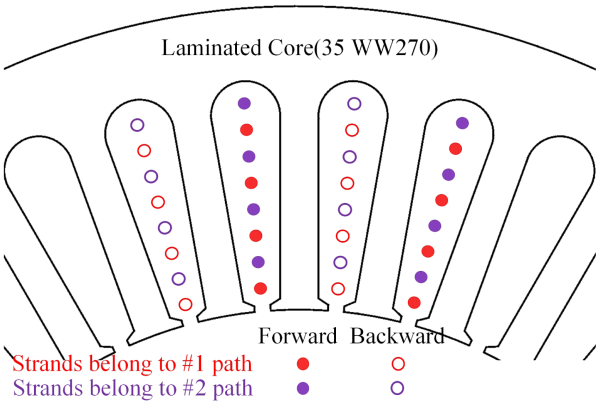

Fig. 3. (Color online) Schematic diagram of tested winding.

Table 1. Specification of tested model.

Parameters	Value
Core outer diameter	180 mm
Core inner diameter	104.3 mm
Core axial length	57.5 mm
Core material	35WW270
Stacking factor	0.94
Strand diameter	1 mm

opening and bottom.

3.1. Extraction of Slot Leakage Inductance

As shown in Fig. 4, a 2-D FE model is built to extract the slot leakage inductances. Neglecting eddy effect in strand, the governing equation of the solving domain can be represented as follows

$$\frac{\partial^2 A_z}{\partial x^2}+\frac{\partial^2 A_z}{\partial y^2}=\mu J_z \tag{9}$$

where μ is the permeability, A_z is the z component of magnetic vector potential and J_z is the z component of current density. The boundary condition of the domain is set as magnetic tangential field condition ($A_z = 0$).

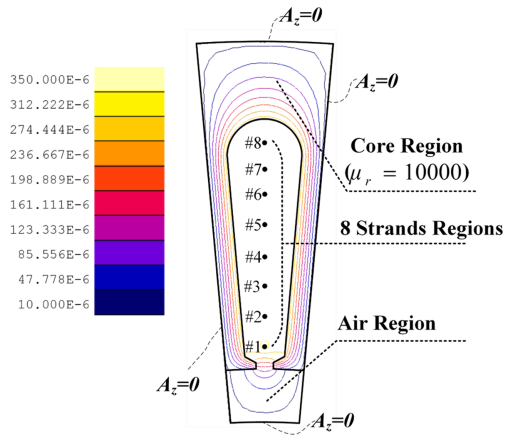

Fig. 4. (Color online) 2-D FE model.

Table 2. Calculated slot leakage inductance matrix (μH).

	1	2	3	4	5	6	7	8
1	0.121	0.115	0.115	0.114	0.114	0.114	0.114	0.114
2	0.115	0.172	0.163	0.162	0.162	0.162	0.162	0.162
3	0.115	0.163	0.214	0.204	0.204	0.204	0.204	0.204
4	0.114	0.162	0.204	0.252	0.241	0.240	0.240	0.240
5	0.114	0.162	0.204	0.241	0.289	0.277	0.276	0.276
6	0.114	0.162	0.204	0.240	0.277	0.321	0.309	0.308
7	0.114	0.162	0.204	0.240	0.276	0.309	0.346	0.333
8	0.114	0.162	0.204	0.240	0.276	0.308	0.333	0.372

The time-harmonic electromagnetic solver is used to obtain the leakage inductances. strands #1~#8 are respectively supplied by 100A (RMS value) current, then the self and mutual inductances can be obtained based on the terminal voltages of all strands. Fig. 4 shows the flux lines distribution when strand #1 is excited. Table 2 shows the calculated inductance matrix of 8 strands, it shows a significant trend that the inductance of the strand close to the slot opening is smaller than that of the strand close to the slot bottom. This results in the uneven current distribution of parallel strands. The self-inductance of strand #8 is about three times larger than that of strand #1. Using formula, the slot leakage inductance matrix $\boldsymbol{L}_p$ (μH) of two paths is calculated as

$$\boldsymbol{L}_p=\begin{bmatrix}12.10 & 12.93\\ 12.93 & 14.66\end{bmatrix} \tag{10}$$

3.2. Extraction of End Leakage Inductance

Figure 5 shows the static 3-D axial symmetric FE model used to calculate the end leakage inductance. The core

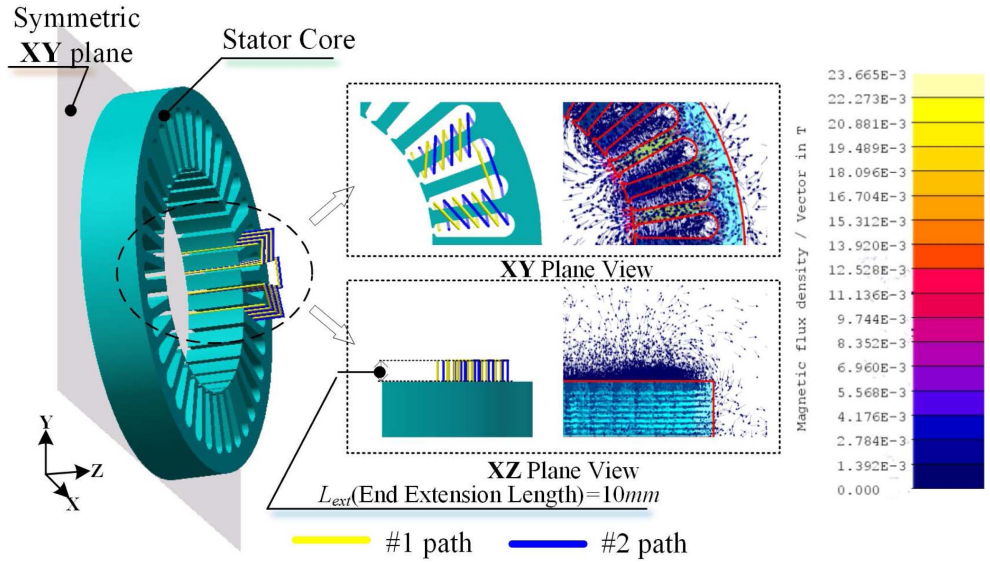

Fig. 5. (Color online) 3-D FE model and flux density vector distribution of end region (③ I_1=1A, I_2=1A)

material is regarded as linear, then the relations between energy (W), current (I) and inductance (L) can be written as

$$\begin{cases} W_1 = \frac{1}{2}L_{11}I_1^2 & \text{Path \#1 excited} \\ W_2 = \frac{1}{2}L_{22}I_2^2 & \text{Path \#2 excited} \\ W_{12} = \frac{1}{2}L_{11}I_1^2 + \frac{1}{2}L_{22}I_2^2 + MI_1I_2 & \text{Path \#1, \#2 excited} \end{cases} \quad (11)$$

where L_{11}. L_{22} denotes the self-inductance of path #1 and path #2, M denotes the mutual inductance. According to the above formula, the end leakage inductance can be obtained by calculating the energy of the air around the end windings under three work conditions (① I_1=1A, I_2=0A; ② I_1=0A, I_2=1A; ③ I_1=1A, I_2=1A). The end extension length L_{ext} represents the single side straight part of end length of one strand as shown in Fig. 5. The self and mutual inductances of the two paths with different end extension lengths (5 mm~15 mm) are shown in Table 3, from which we can see that the end leakage including self and mutual inductance increases with end extension length. The ratio of end leakage inductance to slot leakage inductance is about from 10 % to 16 %.

Table 3. Calculated end leakage inductances.

L_{ext}/mm	L_{11}/μH	L_{22}/μH	M/μH
5	1.494	1.778	1.309
10	1.683	1.945	1.41
15	1.851	2.094	1.495

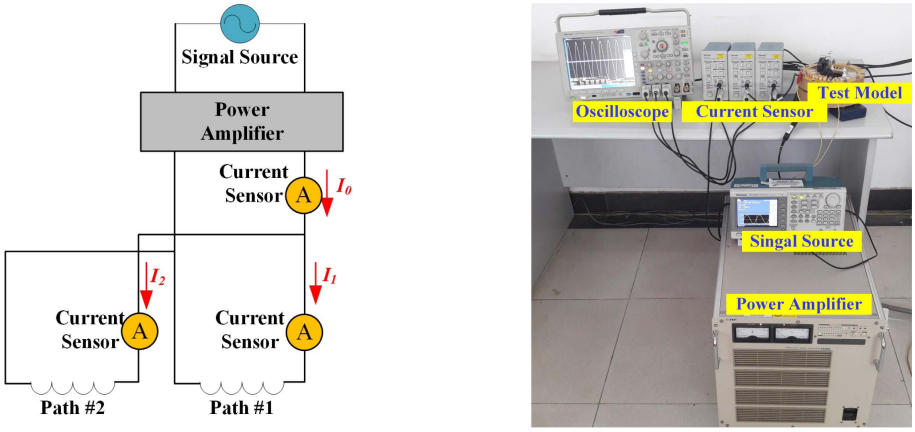

(a) Diagram of experiment (b) Experiment setup

Fig. 6. (Color online) Experiment system.

4. Experimental Validation

The test platform is shown as Fig. 6, the amplifier current is used to supply two parallel paths. Three current sensors are arranged to measure the total current I_0 and two paths currents (I_1, I_2), respectively. The measured total current I_0 is taken as the input of the proposed model, the accuracy of the model will be verified by comparing the calculated path currents with the measured values.

The winding with 5 mm end extension length is taken as the tested winding for verifying the accuracy of the proposed model, the total current is about 0.85A (RMS value) and the frequncy ranges from 200 Hz to 5 kHz. In order to show the accuracy of the improved model, the calculated path currents by two methods are compared with the experimental results, which respectively refer to the methods that ignore and consider the end leakge inductance.

Figure 7 shows the comparison between experimetnal and calculated currents. It shows that the current of path #1 is larger than that of path #2 and the inequality between two paths grows up as the frequency increases. Based on formula (8), the variation of calculated circulating current loss factor with frequency is shown in Fig. 8. It indicates that circulating current effect has been stronger as the frequency increases. By comparing the two calculation methods, it's obvious that the method considering the end leakage inductance is more accurate than the method ignoring end leakage inductance. By modifying the inductance matrix using end leakage inductance, the maximum absolute error of circulating current loss factor has decreased from about 6.6 % to 1.5 %.

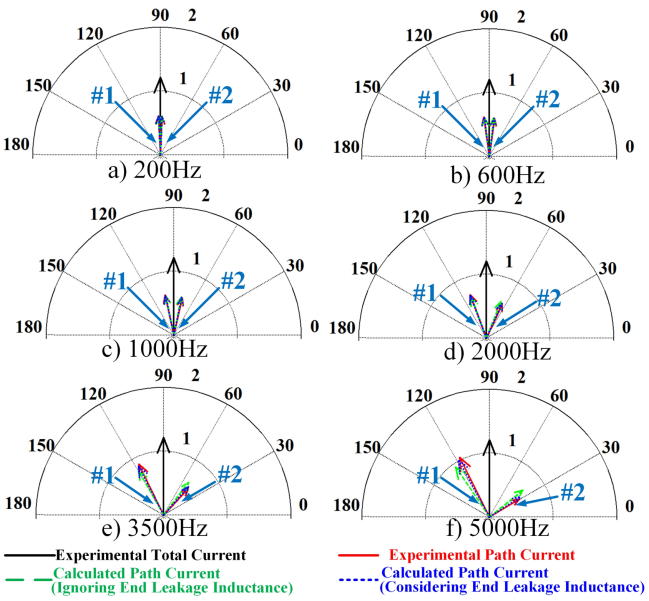

Fig. 7. (Color online) Comparison of current between experiment and calculation.

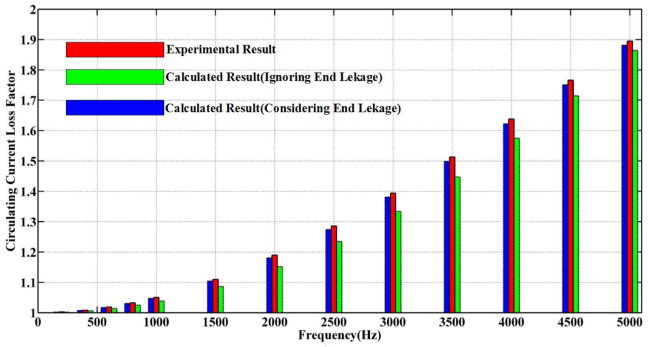

Fig. 8. (Color online) Comparison of loss factor between experiment and calculation.

5. Influence Factors of Circulating Current

The end extension length and temperature influence on circulating current is disscussed in this section.

Firstly, as shown in Fig. 2, several winding schemes with different end extension lengths have been done. Fig. 9 shows the experimental and calculated circulating current factors with different end extension lengths. The end leakage inductance and resistance increase with the increasing of the end extension. Since the resistances of the two paths increases equally, the increasing of the end extension length acts to equalize the current distribution of paths. Experimental results also verify this rule.

Secondly, the temperature effect on the circulating current is investigated by heating up the test model to some fixed temperatures. Fig. 10 shows the experimental and calculated results with different temperatures, from which we can see that the circulating current loss factor decreases as the temperature increases. Similarly, the reason is that the equalized temperature variation of the

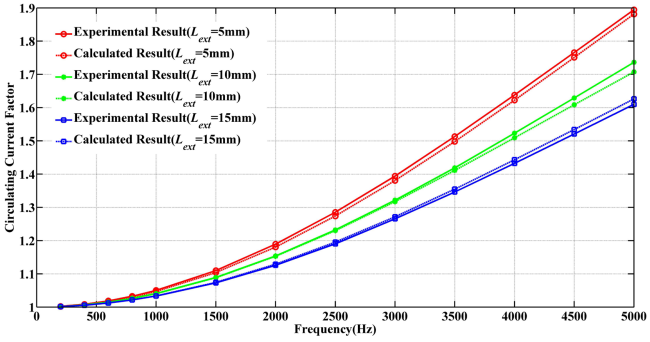

Fig. 9. (Color online) Experimental and calculated loss factor with different end extension lengths.

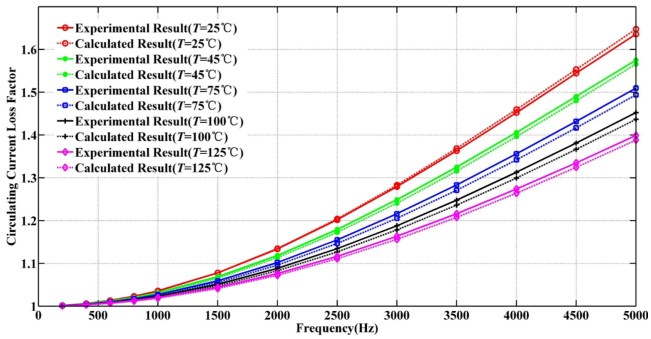

Fig. 10. (Color online) Experimental and calculated loss factor with different temperatures.

two paths leads to the equalized resistance variation, this resuls in the decreasing of current uneven distribution between different paths.

In general, the increasing of both end extension length and temperature will act to the equalize the current distribution, this in turn reduces the circulating current loss factor.

6. Conclusion

This paper has proposed an improved circuit model to calculate the circulating by modifying the impedance matrix with leakage inductance of end winding. The slot and end leakage inductances have been extracted by 2-D and 3-D FEM method, respectively. The accuracy of the method is verified and the maximum absolute error of loss factor is about 1.5 %. Besides, it's found that the circulating current effect becomes weak as the extended end length and temperature increase. The proposed model can be extended to more complex motor with stranded windings.

Acknowledgement

This work was financially supported by the National Natural Science Foundation under Grant 51690181, 51825703.

References

[1] X. Q. Liu, J. C. Fang, and S. Q. Zheng, International Journal of Applied Electromagnetics and Mechanics **48**, 59 (2015).
[2] F. Jiancheng, L. Xiquan, B. Han, and K. Wang, IEEE Trans. Magn. **51**, 1 (2015).
[3] H. Hämäläinen, J. Pyrhönen, J. Nerg, and J. Talvitie, IEEE Trans. Ind. Electron. **61**, 693 (2014).
[4] H. Hamalainen, J. Pyrhonen, and J. Nerg, IEEE Trans. Magn. **49**, 2967 (2013).
[5] M. v. d. Geest, H. Polinder, J. A. Ferreira, and D. Zeilstra, IEEE Trans. Ind. Electron. **61**, 3064 (2014).
[6] M. v. d. Geest, H. Polinder, J. A. Ferreira, and D. Zeilstra, 2013 International Electric Machines & Drives Conference, 340 (2013).
[7] D. Bauer, P. Mamuschkin, H. C. Reuss, and E. Nolle, 2015 IEEE International Electric Machines & Drives Conference (IEMDC), 1247 (2015).
[8] P. B. Reddy and T. M. Jahns, The 2010 International Power Electronics Conference (IPEC), 2181 (2010).
[9] P. B. Reddy, T. M. Jahns, and T. P. Bohn, Proceedings of the 2009 IEEE Energy Conversion Congress and Exposition (ECCE), 1919 (2009).
[10] A. Lehikoinen, N. Chiodetto, E. Lantto, A. Arkkio, and A. Belahcen, IEEE Trans. Magn. **52**, 1 (2016).